Geologica Acta, Vol.11, Nº 3, September 2013, 277-293
DOI: 10.1344/105.000001843
Available online at www.geologica-acta.com

Evidence of extensional metamorphism associated to Cretaceous rifting of the North-Maghrebian passive margin: The Tanger-Ketama Unit (External Rif, northern Morocco)

M. VÁZQUEZ [1,2] **L. ASEBRIY** [3] **A. AZDIMOUSA** [4] **A. JABALOY** [5] **G. BOOTH-REA** [5,6]
L. BARBERO [7] **M. MELLINI** [8] **F. GONZÁLEZ-LODEIRO** [5]

[1] **Andean Geothermal Center of Excellence (CEGA), Universidad de Chile**
Santiago, Chile. E-mail: mmvazquez@ugr.es

[2] **Department of Geology, Universidad de Chile**
Santiago, Chile. E-mail: mvazquez@ing.uchile.cl

[3] **Institut Scientifique, B.P. 703, Université Mohammed V**
Agdal-Rabat (Morocco). E-mail: asebriy@israbat.ac.ma

[4] **Laboratoire LGA, Faculté des Sciences, Université Mohammed I**
Oujda (Morocco). E-mail: azdi61@yahoo.fr

[5] **Departamento de Geodinámica, Facultad de Ciencias, Universidad de Granada**
C/Fuentenueva s/n. 18071, Granada Spain

[6] **Departamento de Geodinámica, Instituto Andaluz de Ciencias de la Tierra (IACT), CSIC-Universidad de Granada**
Facultad de Ciencias, 18002, Granada (Spain).E-mail: gbooth@ugr.es

[7] **Departamento de Ciencias de la Tierra, Facultad de Ciencias del Mar y Ambientales, Universidad de Cádiz**
11510 Puerto Real, Cádiz (Spain). E-mail: luis.barbero@uca.es

[8] **Dipartimento di Scienze della Terra, Università di Siena**
Via del Laterino 8, 53100 Siena (Italy). E-mail: mellini@unisi.it

ABSTRACT

The distribution pattern of diagenetic conditions to very low-grade metamorphism in the eastern Rif has been determined based on a study of clay-mineral assemblages and illite crystallinity of Mesozoic metapelites. Low-grade conditions were reached in marbles and also in the Beni-Malek serpentinites, as suggested by the mineral assemblages present in the marbles and antigorite growth in serpentinites. Previous thermochronological data are based on i) $^{40}Ar/^{39}Ar$ in amphiboles from greenschists; and ii) K/Ar in white micas from metasandstones, and iii) fission tracks in apatites and zircons from metasandstones. These data indicate a Late Cretaceous age (~80Ma) for the very low- to low-grade metamorphism. We propose an evolutionary model for the Tanger-Ketama Unit consisting of a Lower Cretaceous sequence deposited in half-graben basins over an exhumed serpentinized mantle in a setting similar to the West Galician non-volcanic margin. The sediments underwent diagenesis to very low-grade metamorphism under relatively high heat flow in this extensional setting. Miocene contractional deformation of the Tanger-Ketama Unit resulted in a penetrative crenulation cleavage associated to asymmetric inclined folds. This crenulation developed, mostly by solution-transfer processes, without significant mineral growth. Miocene metamorphism reset the apatite fission-tracks, but metamorphic conditions were not high enough to reset either the K/Ar ages or the zircon fission tracks.

KEYWORDS **Low-grade extensional metamorphism. Illite crystallinity. Kübler index. Tanger-Ketama unit. External Rif. Northern Morocco.**

INTRODUCTION

Diastathermal or extensional metamorphism has been described in certain ancient continental areas that have experienced considerable thinning and subsidence (Robinson, 1987; Robinson and Bevins, 1989; Merriman, 2005). Extensional metamorphism in these cases is characterized by very low- to low-grade conditions and is caused by heating at the base of the basin related to thermal blanketing by the overlying sedimentary sequence and to the high heat flow characteristic of extensional settings. The thick sedimentary cover acts as an insulating, low-conductivity layer inhibiting advective heat transfer (Zhang, 1993). This is especially the case when the sedimentary cover consists of impermeable pelitic facies that do not permit advective heat transfer. The Palaeozoic Welsh Basin (United Kingdom) is one of the type examples of a diastathermal setting. Regional studies of illite crystallinity from metapelites in this basin (*e.g.* Merriman and Roberts, 1985; Roberts and Merriman, 1985; Robinson and Bevins, 1986) established the overall pattern of metamorphism across the basin, characterized by deeper diagenesis along its margin to epizonal conditions in the centre. Since metamorphic grade increases with strata age, Robinson and Bevins (1986) suggested that depth of burial was the dominant control on the metamorphic pattern when shale sequences are buried in a passive margin setting (Merriman and Frey, 1999; Merriman, 2005).

Late Jurassic to Early Cretaceous extension also occurred in several basins around Iberia and the Tethys (Casas *et al.*, 2000; Mata *et al.*, 2001; Goldberg *et al.*, 1986, 1988), in some cases leading to the exhumation of subcontinental mantle, as in the non-volcanic West Iberian and Tethyan passive margins in the Alps and the Pyrenees (Golberg *et al.*, 1986; Montigny *et al.*, 1986; Fabriés *et al.*, 1998; Pérez-Gussinyé and Reston, 2001; Wilson *et al.*, 2001, and references therein). Subcontinental mantle exhumation also occurred in the North-Maghrebian passive margin, resulting in the exposure of the Beni-Malek serpentinites and other small serpentinitic bodies (Michard *et al.*, 1992; 2007). Geophysical studies suggest the existence of at least two 20x10km-sized peridotitic bodies below the eastern Rif (Elazzab *et al.*, 1997).

Extensional metamorphism in regions that have undergone later orogenesis can easily be overprinted by tectonic thickening-related metamorphism. This is probably why pre-orogenic extensional metamorphism is poorly documented in passive margins presently forming part of orogenic belts such as the Alps or the Betics-Rif.

In this paper, we present evidence for the occurrence of extensional metamorphism associated with the development of the Mesozoic North-African passive margin and the exhumation of subcontinental serpentinized mantle in the very low- to low-grade metamorphic rocks of the Tanger-Ketama Unit (Rif Cordillera, North Africa). We have studied this low-grade metamorphism and determined its relationship with the pre-orogenic extensional structure of the North-African passive margin. We then examine these results in the light of previous thermochronological data and discuss the tectonic implications for the regional evolution of the Rif Cordillera.

GEOLOGICAL SETTING

The Rif Belt (northern Morocco) and the Betics (southern Spain) are the western arcuate termination of the Alpine Mediterranean orogen (Fig. 1) produced by the convergence of the African and Eurasian plates since the Late Mesozoic (*e.g.* Dewey *et al.*, 1989; Jolivet *et al.*, 2003; Chalouan and Michard, 2004). The Rif Belt forms an arc-shaped mountain belt fringing northern Africa, extending from Morocco to the west to Algeria to the east (Tell Mountains).

Three major zones are usually distinguished in the Rif Belt: the Internal Zones, the Maghrebian Flyschs, and the External Zones (Figs. 1; 2). The Internal Zones are part of the Alborán Domain according to Balanyá and García-Dueñas (1987). These Internal Zones have been interpreted as part of an allochthonous terrane formed by a stack of hinterland metamorphic units (Andrieux *et al.*, 1971; Balanyá and García-Dueñas, 1987) that underwent subduction-collision processes (*e.g.* Azañón and Crespo-Blanc, 2000; Faccenna *et al.*, 2004; Michard *et al.*, 2006; Booth-Rea *et al.*, 2007). The Maghrebian Flyschs are overthrust by the Internal Zones except for some outcrops on top of the Alborán Domain. The tectonic units of the Maghrebian Flyschs are composed of Lower Jurassic to Oligocene sediments

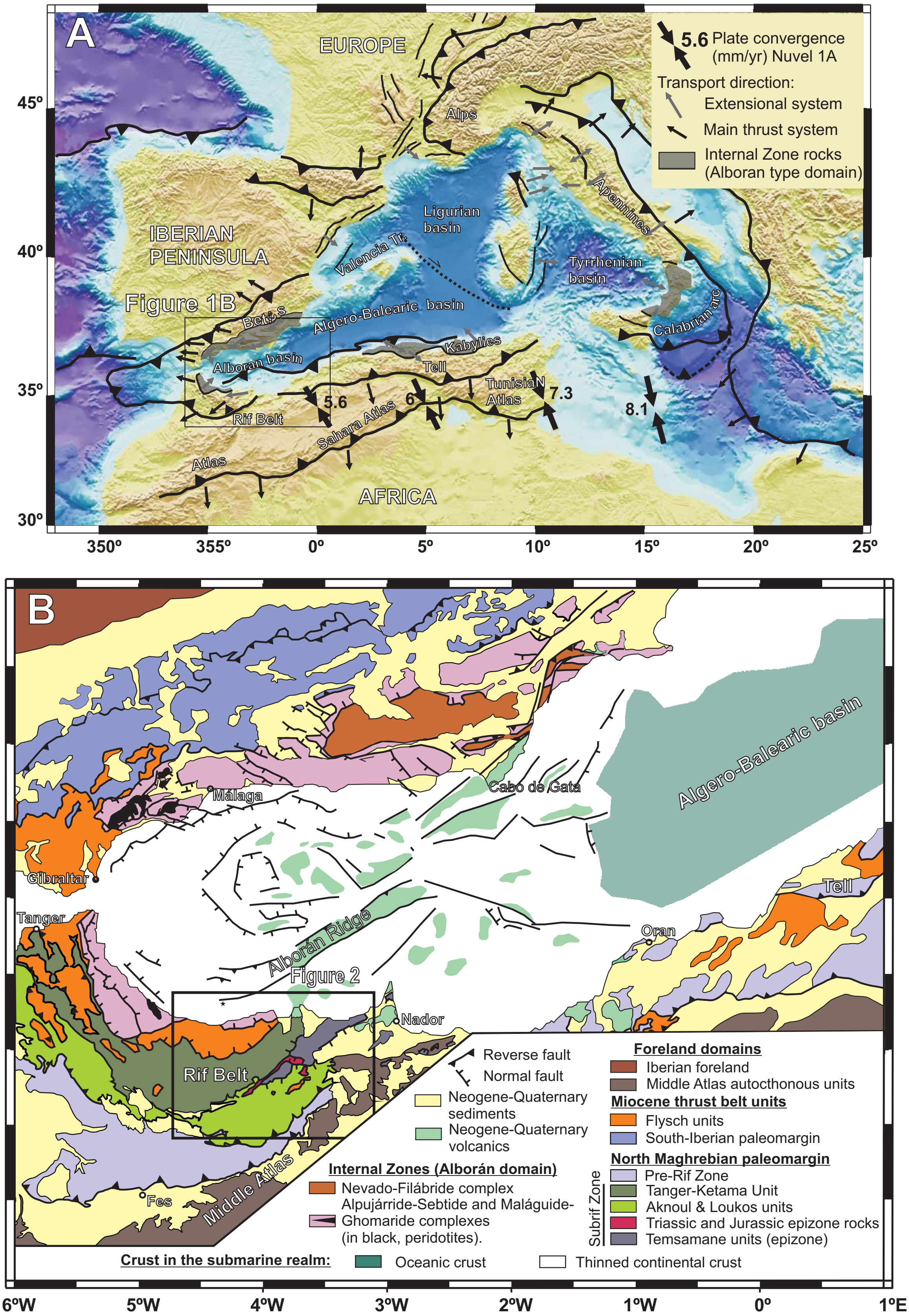

FIGURE 1 A) Geological sketch of the Western Mediterranean. Rectangle marks the location of Figure 2. B) Geological sketch of the Rif Belt.

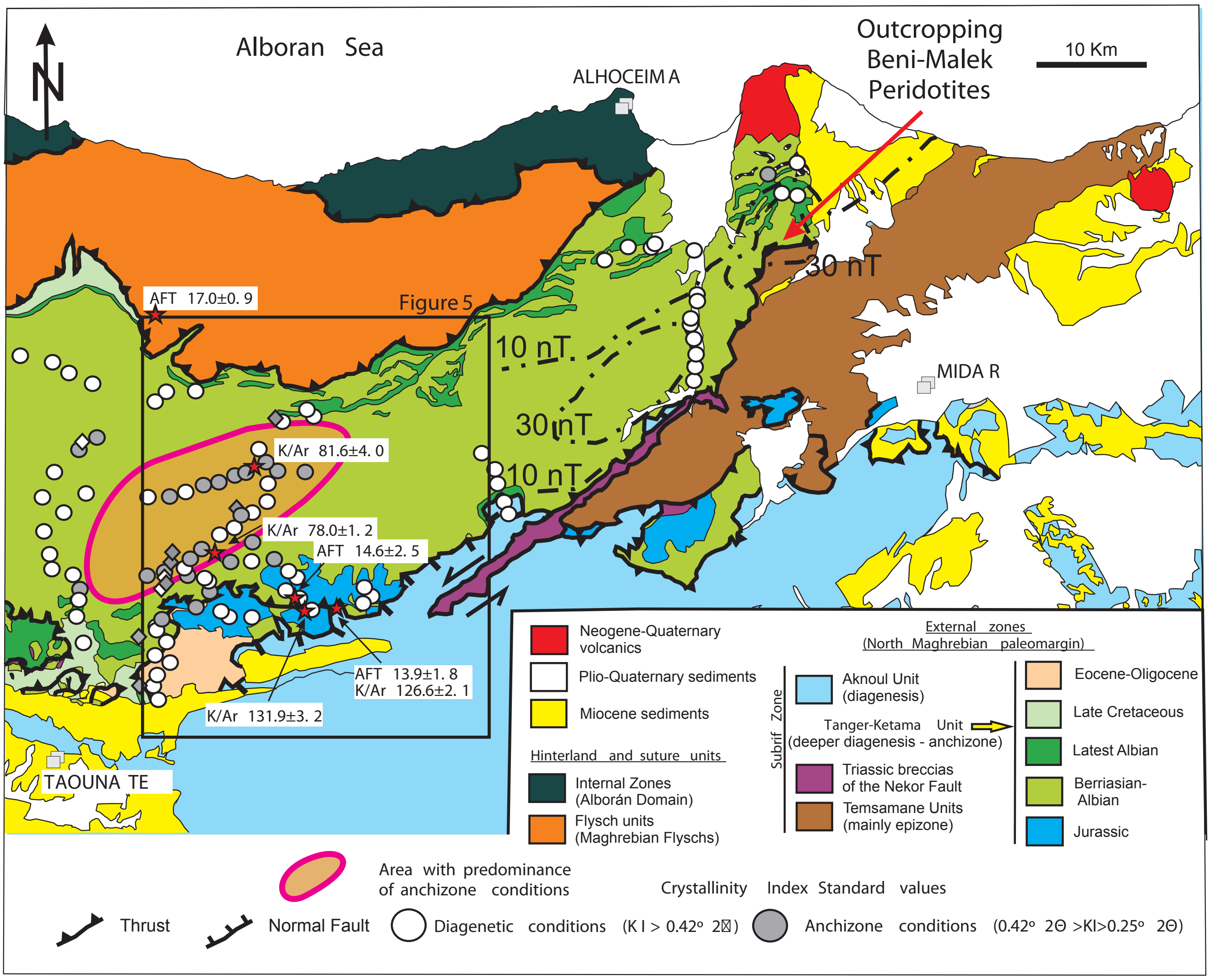

FIGURE 2 | Geological map of the eastern Rif with the location of the samples mentioned in the study. Circles represent the samples from Leikine *et al.* (1991) with the new Calibration International Standard value calculated in this work (Table I, electronic appendix available at www.geologica-acta.com), and diamonds represent the new samples from this work (Table 1). The area outlined in magenta indicates the zone with anchizone conditions. Stars indicate the location and age of the K/Ar (K/Ar) and apatite fission-track (AFT) data from Azdimousa *et al.* (1998, 2003). Dashed and dotted black lines represent the isolines of the magnetic anomaly at 10 nT and 30 nT respectively; the latter roughly corresponds with the limits of the modeled ultramafic bodies below the Eastern Rif Belt (Elazzab *et al.*, 1997).

with Lower Cretaceous and Oligo–Miocene turbiditic levels. They represent deep-seated sediments deposited on highly thinned continental crust or on oceanic crust located between the African palaeomargin and the Alborán Domain (Durand-Delga *et al.*, 2000).

The External Zones are interpreted as the North African (Maghrebian) passive margin overthrust by the Internal Zones. The External Zones are mainly formed by Mesozoic and Cenozoic sediments and also include minor alkaline intrusive rocks and serpentinites. This palaeomargin underwent different stages of subsidence, mainly during the Cretaceous, and is characterized by olistostrome-rich sequences with fragments of limestones, shales, gypsum bodies from the Mesozoic and Cenozoic cover sequences, and fragments of schists and metaconglomerates from the Palaeozoic sequences of the African basement, with significant lateral variations in thickness (Lespinasse, 1975; Asebriy, 1984; Ciszak *et al.*, 1986; Asebriy *et al.*, 1987; Ciszak, 1987; Kuhnt and Obert, 1991).

The External Zones are themselves composed of two structural zones: the Sub-Rif Zone and the Pre-Rif Zone (Asebriy *et al.*, 1987). The Sub-Rif Zone includes the Intra-Rif and Meso-Rif zones as defined by Durand-Delga *et al.* (1962). The Pre-Rif Zone, to the south of the Rif Belt, is a sedimentary complex of olistostromes with Palaeozoic to Cenozoic blocks in a matrix mainly composed of Tortonian marls (Sutter, 1980; Vidal, 1971; Leblanc, 1975-1979; Bourgois, 1977).

The Sub-Rif Zone (Asebriy *et al*., 1987) is composed of diagenetic to low-grade metamorphic rocks deformed under brittle to ductile conditions (Andrieux, 1971; Frizon de Lamotte, 1985; Michard *et al*., 1992; Asebriy, 1994; Asebriy *et al*., 2003; Azdimousa *et al*., 1998, 2007). It crops out in the central part of the chain and is characterized by a continuous Lower Jurassic to Cretaceous, mostly pelitic, sedimentary sequence. Several tectonic units include Cenozoic sediments and a few alkaline intrusions of Mesozoic diorites. These alkaline intrusions were dated by K-Ar methods as Middle Jurassic (166 ± 3Ma), indicating extensional tectonics in the Callovian–Oxfordian (Harmand *et al*., 1988; Asebriy, 1994). In the eastern Rif Belt, the Sub-Rif Zone is composed of two groups of tectonic units, the Tanger-Ketama Unit and the Temsamane Units (Fig. 2). The former unit thrusts over the latter one.

The Tanger-Ketama Unit has variable metamorphism ranging from very low to low grade (Leikine *et al*., 1991). These authors observed as the main mineral assemblages muscovite, paragonite, albite and calcite, and also interstratifications such as illite/smectite and paragonite/muscovite. This metamorphism has been dated by K/Ar mica ages and zircon fission tracks (Azdimousa *et al*., 1998, 2003). K-Ar ages range from 131.9±3.2Ma to 126.6±2.1Ma (Hauterivian–Barremian ages) in the Jurassic rocks, and 81.6±4.0Ma to 78.0±1.2Ma (Campanian) in the Lower Cretaceous rocks (Azdimousa *et al*., 1998, 2003). These ages are considered to be related to the cooling ages determined by fission-track dating in the same rocks (Azdimousa *et al*., 1998, 2003) (Fig. 2). The metamorphism affecting Lower Cretaceous rocks is dated at 75 to 85Ma by zircon fission tracks. These authors attribute these ages to the total resetting of the zircon grains at temperatures of around 300ºC (Azdimousa *et al*., 1998, 2003). However, the temperature of the metamorphism that affected the Upper Jurassic sequence is not as well constrained by fission tracks since the zircons show older ages than the depositional ages, indicating maximum temperatures below 200°C. Apatite fission-track ages range from 13.9±1.8Ma to 17.0±2.4Ma, suggesting that the rocks entered the Complete Annealing Zone of apatite (T>110ºC) and cooled below 110ºC during the Burdigalian to the Langhian.

Negro (2005) and Negro *et al*. (2007, 2008) estimated temperatures of around 350±30ºC and pressures of 7–8kbar for the main metamorphic stage in the Northern Temsamane Unit (Fig. 2). The Central and Southern Temsamane units show lower temperatures and pressures. $^{40}Ar/^{39}Ar$ dating on micas is scarce and results range widely between 8 and 23Ma (Monié *et al*., 1984; Negro, 2005; Negro *et al*., 2007, 2008).

LITHOSTRATIGRAPHIC SEQUENCE AND STRUCTURE OF THE TANGER-KETAMA UNIT

The main outcrop of the Tanger-Ketama Unit (Andrieux, 1971; Gübeli *et al*., 1984) corresponds to a major thrust sheet whose basal surface crops out south of Alhoceima (just south of the Beni-Malek Peridotites in Fig. 2) over the Temsamane units. Towards Taounate, the main thrust sheet is duplicated by a secondary thrust surface that crops out in four tectonic windows (Fig. 2). The lithological sequence of the upper thrust sheet comprises two formations present throughout the entire outcrop: a lower Formation (Fm.) (around 500 metres thick) of whitish carbonate shales with levels of limestones and sandstones dated as Berriasian–Hauterivian followed upsection by around 500 metres of Aptian–Lower Albian dark shales with sandstone layers (Fig. 3A) (Azdimousa *et al*., 1998; 2003).

The Lower Cretaceous sediments of the upper thrust sheet of the Tanger-Ketama Unit overlie two very different types of rocks. In the western and central part of the upper thrust sheet, the Early Cretaceous metapelites overlie around 500m of Jurassic carbonate and pelitic formations (Asebriy *et al*., 1992). However, in the east of the Tanger-Ketama Unit outcrops, the Cretaceous sedimentary rocks are deposited over the ultramafic rocks of the Beni-Malek massif (Michard *et al*., 1992).

The Beni-Malek peridotite forms a lens-shaped body approximately 400m thick and 2km long (Choubert *et al*., 1984; Michard *et al*., 1992) (Fig. 2). It mainly consists of serpentinized spinel lherzolites (Michard *et al*., 1992), including the presence of occasional pyroxenite layers (spinel websterites). The lerzholites are strongly sheared with domains having fine-grained olivine (Fig. 3G), whereas the serpentinites also include small shear zones and brittle faults with striations. The peridotite body is located over an adjacent 10–20m thick strongly sheared marble layer that has been attributed to the Jurassic. The marbles are mylonitic rocks with a strong planar-linear fabric and include sheared serpentinite clasts. The mineral assemblage of the marbles includes calcite, phlogopite, phengite, and serpentine polymorphs. In the Ait Amrâne klippe, west of Midar (Fig. 2), amphibolites with actinolite, albite, biotite, epidote, and titanite have been found within similar marbles. These assemblages correspond to low-grade metamorphism (greenschist facies) and indicate that the Mesozoic sequence reached temperatures lower than 500ºC. The metamorphic peak was reached at 80Ma according to the $^{40}Ar/^{39}Ar$ radiometric ages on amphiboles determined in the greenschists within the Jurassic marbles (Jabaloy *et al*., 2012).

Lower Cretaceous slates, phyllites, and quartzites of the Tanger-Ketama Unit overlie the peridotitic body, without

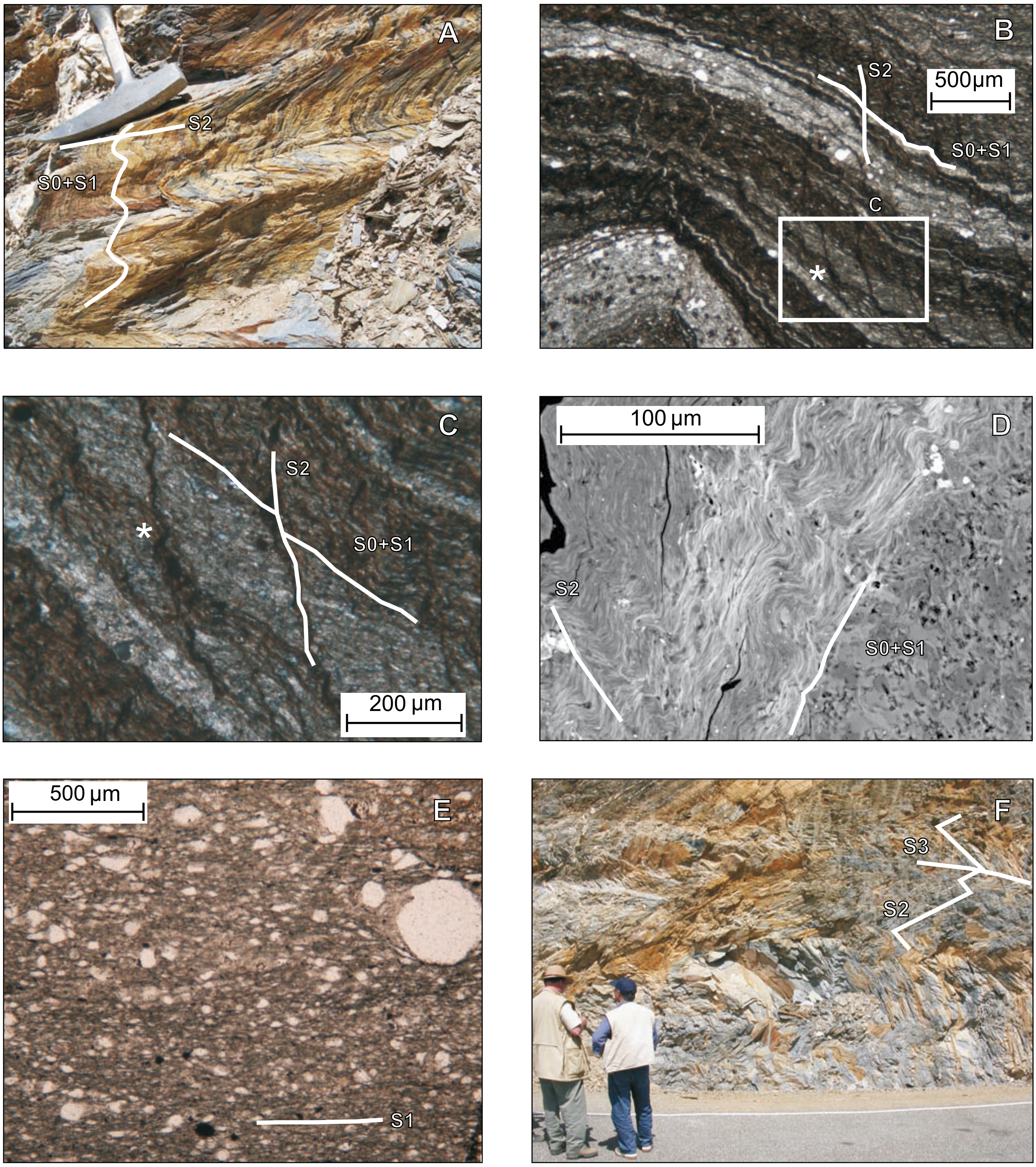

FIGURE 3 A) View of an outcrop of the Aptian–Lower Albian pelites of the Tanger-Ketama Unit with the two foliations described in the text (S1 subparallel to S0 and S2). B) Thin-section views of sample KET-4, which corresponds to the Berriasian–Hauterivian pelites of the Tanger-Ketama Unit. The sample has two foliations: S1 subparallel to S0 is a bedding-parallel foliation, and S2 is a discrete crenulation cleavage cutting the sedimentary layers at points marked with *. C) Close-up of sample KET-4 — its location corresponds to the rectangle marked in B. D) SEM view of sample KET-4 corresponding to the Berriasian–Hauterivian pelites; to the right there is a layer of calcite + quartz + phyllosilicates marking the lithological contact (S0). To the left there is a pelitic layer with chlorites (white) and illites (grey). The crystals of the phyllosilicates defining the S1 are parallel to each other and parallel to the S0. S2 can be observed as an incipient zonal crenulation cleavage. E) Thin-section view of the S1 slaty cleavage in sample KET-8 with a CIS value of 0.37° 2Θ corresponding to the Aptian–Lower Albian pelites of the Tanger-Ketama Unit. F) Outcrop of the Berriasian-Hauterivian phyllites of the affected by F3 open folds with a slow-dipping S3 foliation. G) Thin-section view of a protomylonite corresponding to the sheared lerzholites in the Beni Malek ultramafic body: olivine (ol), orthopyroxene (OPx). H) Thin-section view of the serpentinites within the Beni Malek ultramafic body showing the mesh structure transformed into the fine-grained aggregate of antigorite (antg).

the presence of a fault surface separating the different kinds of rocks (Michard *et al.*, 1992). The presence of sandstones with mafic and ultramafic clasts within the Lower Cretaceous sedimentary rocks, southeast of the Beni-Malek massif (Michard *et al.*, 1992; Chalouan *et al.*, 2008), supports the location of these rocks on the seafloor during the Lower Cretaceous. Elazzab *et al.* (1997) studied the regional aeromagnetic anomaly of the area, proposing that there are another two major ultramafic bodies (around 20x10km^2) below the eastern outcrop of the Tanger-Ketama Unit (Fig. 2). Michard *et al.* (1992) and Chalouan *et al.* (2008) interpreted the Beni-Malek ultramafic body as a sliver of serpentinite that originated from an Alpine-type non-volcanic continental margin that developed in the Mesozoic Eastern Rif passive margin (Wilson *et al.*, 2001; Boillot and Froitzheim, 2001). Tectonic denudation of mantle rocks occurred in the very distal portion of this margin, in the continent-ocean transition. This sliver was later incorporated into the present thrust pile during the Iberian-African Tertiary collision.

The upper part of the lithological sequence of the upper thrust sheet of the Tanger-Ketama Unit is composed of around 50 metres of Latest Albian green pelites, followed upsection by about 600m of detrital and carbonate formations ranging from the Late Cretaceous to the Eocene.

The lower thrust sheet of the Tanger-Ketama Unit that crops out in the four tectonic windows north of Taounate has a very similar lithological sequence, but it lacks ultramafic rocks and also includes unconformable Upper Oligocene conglomerates, sandstones, and shales, dated with fossils (Asebriy *et al.*, 1992; Asebriy, 1994). The conglomerates include clasts from the Mesozoic Tanger-Ketama sequence (Figs. 4; 5) and are affected by a spaced cleavage and thrust by the upper thrust sheet during the Miocene (Asebriy *et al.*, 1992; Asebriy, 1994).

ANALYTICAL METHODS

X-ray diffraction (XRD)

The sequence of the Tanger-Ketama Unit was studied by X-ray diffraction (XRD) in order to determine mineral assemblages and metamorphic conditions. Ten unaltered shale and slate samples were carefully collected and washed; after coarse crushing, homogeneous rock chips were used for XRD preparation. Whole-rock samples and the clay fraction (<2µm) were studied using a Philips PW 1710 X-ray diffractometer with Cu-Kα radiation, graphite monochromator, and automatic divergence slit (Department of Mineralogy and Petrology, University of Granada, Spain).

The <2µm fractions were separated by repeated extraction of supernatant liquid subsequent to settling. Orientated aggregates were prepared by sedimentation on glass slides. Some samples were ethylene-glycol (EG) treated to corroborate the identification of smectite and/or illite-smectite mixed-layers. Preparations of samples and experimental conditions for illite crystallinity (Kübler Index) measurements were carried out according to IGCP 294 IC Working Group recommendations (Kisch, 1991). The Crystallinity Index Standard scale considered for the calibration of the Kübler Index was the original one proposed by Warr and Rice (1994) as no differences in the measurements were found using their inter-laboratory standards and those proposed by Kisch *et al.* (2004). Our Kübler Index measurements (y) were transformed into Crystallinity Index Standard values (x) using the equation $y = 1.6583\,x - 0.0484$ ($r = 0.9996$). The Kübler Index values were measured for the <2µm fractions and

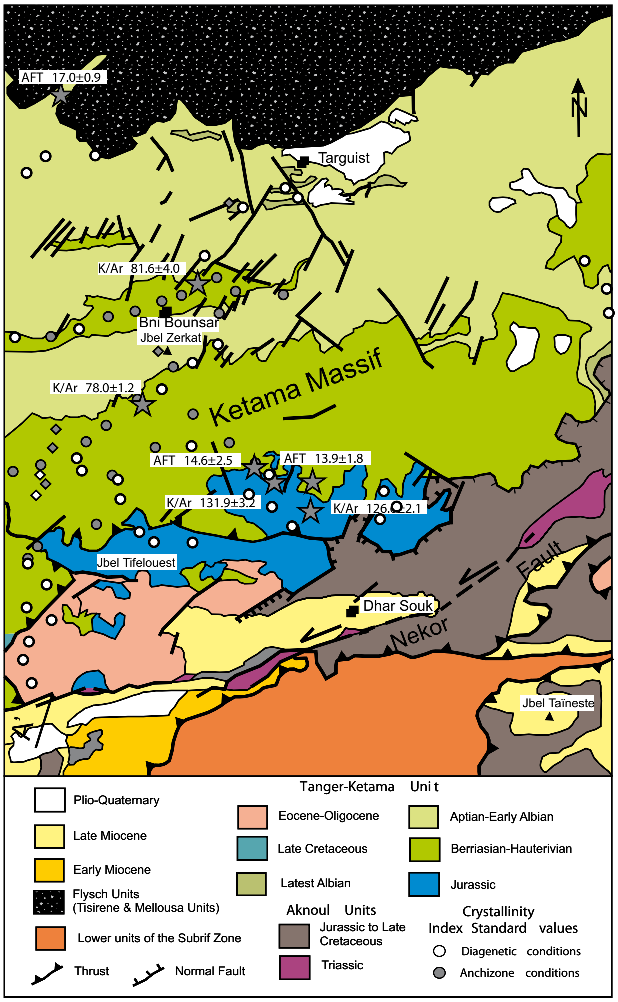

FIGURE 4 | Geological map of the central part of the Tanger-Ketama Unit (see location in Fig. 2), with the locations of the samples: Circles represent the samples from Leikene *et al.* (1991) with the new Crystallinity Index Standard value calculated in this work, and diamonds represent the new samples from this work.

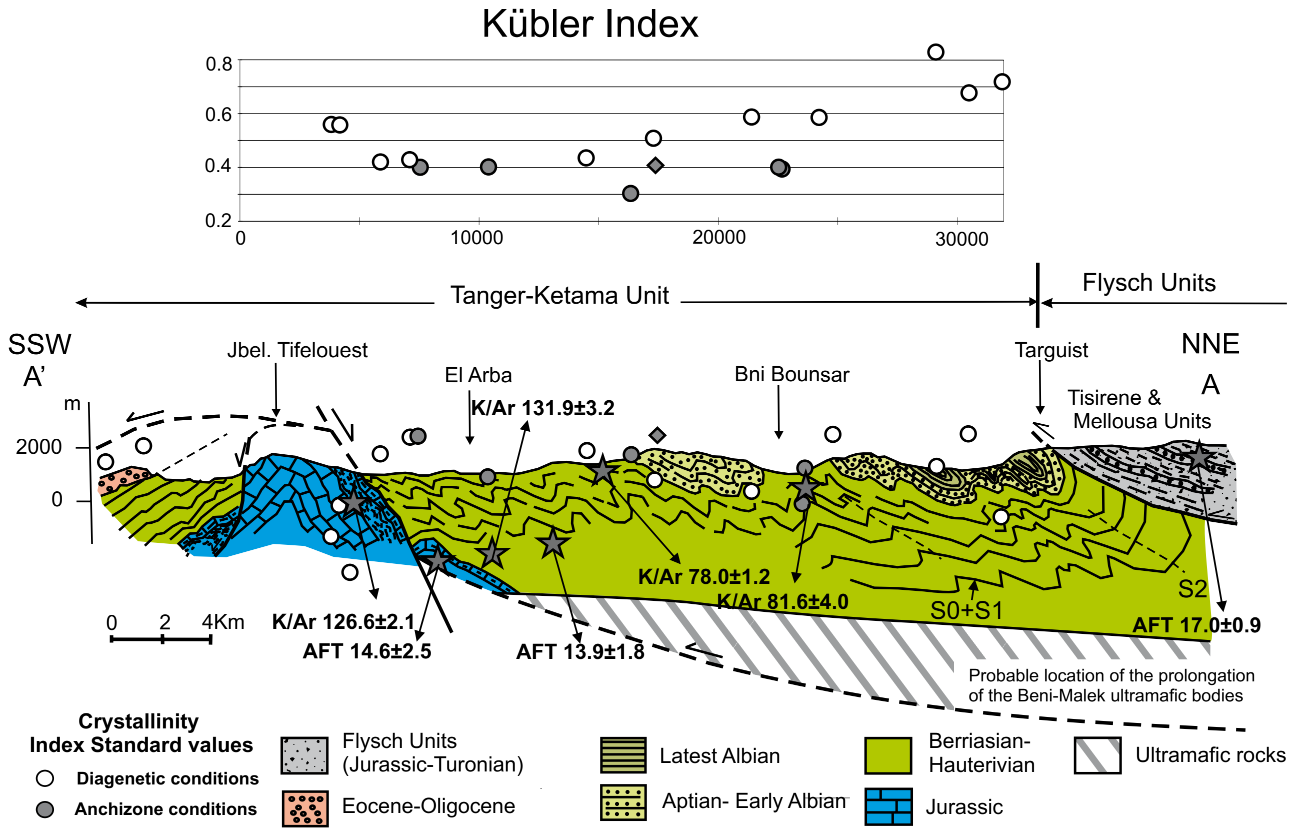

FIGURE 5 | Cross-section of Tanger-Ketama Unit showing the distribution pattern of Crystallinity Index Standard Kübler Index values across the unit. Only those samples with a normal distance of less than 2 km to the profile surface have been represented. Circles represent the samples from Leikene *et al.* (1991) with the new Crystallinity Index Standard value calculated in this work, and diamonds represent the new samples from this work. The probable location of the prolongation of the Beni-Malek ultramaphic bodies is based on the aeromagnetic data from Elazab *et al.* (1997).

for the bulk-rock samples. The b cell parameters of micas and chlorites were obtained from the 060 peaks measured on rock slices cut normal to the sample foliation. For all spacing measurements, quartz from the sample itself was used as the internal standard.

The Crystallinity Index Standard value of the illite crystallinity index from the samples studied by Leikine *et al.* (1991) have been added to our data in order to compile more information about variations in this parameter within the central and eastern outcrops of the unit (Table I). The experimental conditions used by Leikine *et al.* (1991) for illite crystallinity (Kübler Index) measurements were different from those included in the IGCP 294 IC Working Group recommendations (Kisch, 1991), the calibration most commonly used currently. In order to correct for this fact, we took the samples studied by Leikine *et al.* (1992) that were stored at the Institut Scientifique from the University Mohammed V of Agdal-Rabat (Morocco). We selected fifteen samples with very different original Kübler Index values from the original sampling and determined their Crystallinity Index Standard values in the Granada Laboratory according to IGCP 294 IC Working Group recommendations (Kisch, 1991) (Fig. 6). An excellent linear correlation was obtained between the new Crystallinity Index Standard data and the original Kübler Index values from Leikine *et al.* (1991), using the equation $y= 0.9489x + 0.1005$ ($r=0.9479$) (Fig. 6). We then calculated 97 Crystallinity Index Standard values for all the Kübler Index data from Leikine *et al.* (1991) (Table 1) using this equation. The errors between the real Crystallinity Index Standard data and those calculated from the data published by Leikine *et al.* (1991) are not higher than 0.09º2Θ, and most are in the range of 0.02–0.01º2Θ (Fig. 6).

Electron Microscopy

Following the optical studies, representative samples were selected for electron microscopy study on the basis of the observed foliations and bedding. Thin-section compositional images of backscattered electrons were obtained with an Environmetal Scanning Electron Microscope (ESEM) Quanta 400, FEI, equipped with a backscattered electron Solid State Detector (SSD), using an acceleration voltage of 25kV. Semiquantitative mineral

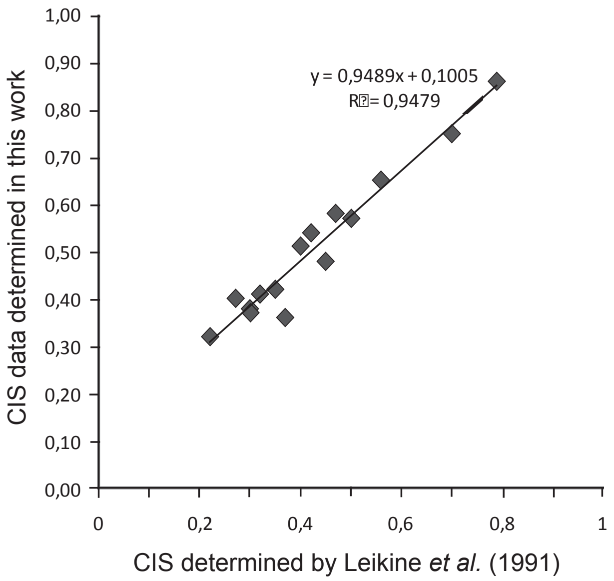

FIGURE 6 | Correlation between the Crystallinity Index Standard (CIS) values of the Leikine *et al.* (1991) samples obtained in the Granada Laboratory for this work and their old Kübler Index previously published.

microanalyses were performed using an Energy Dispersive X-ray instrument (EDAX) attached to the ESEM.

As serpentine polymorphs cannot be differentiated by XRD, High-Resolution Transmission Electron Microscopy (HRTEM) was used in order to unambiguously identify the serpentine mineral assemblages. Appropriate areas of thin sections from the Beni-Malek serpentinites were selected by gluing copper rings on samples. After detachment, they were ion-thinned and carbon-coated for TEM observation. Samples were examined using a JEOL 2010 microscope (at the University of Siena) operated at 200kV and equipped with a Link energy-dispersive spectrometer. Lattice images were obtained using reflections with interplanar spacing greater than 2Å.

RESULTS

Illite crystallinity

The XRD data of the Tanger-Ketama Unit show that quartz, calcite, chlorite, and muscovite are the principal phases in all samples (Table 1). Na/K mica and paragonite have been detected in some samples and show complex clay-mineral assemblages. Illite crystallinity was measured in the samples before and after glycolation. The illite crystallinity in samples KET-2 and KET-4 is considerably higher in the ethylene-glycolated samples, indicating the presence of illite-smectite (I/S) mixed-layers (R3). The co-existence in KET-4 of illite-smectite and Na-K micas, which are thermodynamically incompatible phases, could be due either to a retrograde-diagenetic origin for illite-smectite (according to Nieto *et al*., 2005) or to the presence of detrital components of Na-K micas. Therefore, the Kübler Index has not been considered in this study. Six out of ten samples confirm anchizone metamorphic conditions (0.33 to 0.41º 2Θ), and samples KE-3, KE-6, KET-10, and TAO-4 show a diagenetic grade (0.47 to 0.57 Δº 2Θ). The muscovite b parameter shows extremely homogeneous values from 8.989 to 8.999Å (Table 1). Due to crystal-chemical reasons, the b parameter is closely related with the phengitic content of micas, which in turn depends on their Fm. pressure (Massonne and Schereyer, 1987; Massonne and Szpurka, 1997). The described values indicate very low phengitic contents and therefore low-pressure conditions. Sassi and Scolari (1974) and Guidotti and Sassi (1986) assigned to this b parameter value a pressure that is partly dependent on temperature, but never higher than 2kbar. The Kübler Index distribution pattern shows that metamorphism in the Tanger-Ketama Unit reached variable conditions. The Kübler Index distribution records anchizone conditions in a small area in the central part of the unit, which crops out 20km northeast of Taounate. This distribution also indicates deeper diagenetic conditions in the northern and southern borders of the study area (Figs. 2; 4). This Kübler Index distribution pattern shows a region of maximum metamorphic grade with an ENE-WSW trend in the central outcrops. Figure 5 shows only those samples with a maximum normal distance to the cross-section surface of 2km. In the figure, the Kübler Index clearly decreases towards the centre of the unit, where the lowest values (0.32º2Θ) occur. The lowest-grade rocks that reached deeper diagenetic conditions are found in the southern and northern outcrops of the Tanger-Ketama Unit, affecting Jurassic and Uppermost Albian samples, respectively. As mentioned above, there are unconformable Oligocene conglomeratic deposits with metamorphic clasts forming the uppermost sedimentary Fm. of the lower thrust sheet of the Tanger-Ketama Unit. The clays in the matrix of these Oligocene conglomerates have Kübler Index values ranging from 0.46 to 0.85º2Θ, characteristic of diagenetic conditions. The lowest value (0.46º2Θ) corresponds to sample TAO- 4 with smectites and illite-smectite mixed-layers. These Oligocene conglomerates lie unconformably over Jurassic and Lower Cretaceous rocks of the lower thrust sheet, and also underwent diagenetic conditions (Figs. 4; 5). Therefore, Miocene thrusting of the upper Ketama unit over the Oligocene conglomerates did not contribute to anchizonal metamorphism in the Ketama unit (Asebriy *et al*., 1992; Asebriy, 1994).

Structure

The rocks of the Tanger-Ketama Unit experienced two deformation phases (Andrieux, 1971) producing two cleavages. The oldest fabric is a slaty cleavage (S1) parallel to the lithological layering, defined by the growth

TABLE 1 | Crystal-chemical parameters and bulk mineralogy of the Tanger-Ketama Unit. See location in Figure 2

		White Mica						*Chlorite*			
		d $_{001}$Å		b Å	Illite "Crystallinity" (KI) "CIS" scaleº 2 Θ			d $_{001}$ Å		b Å	Mineral composition Qtz, Cc, Ms, Chl (all samples)
Sample	Age	<2 µm	Total		<2µm	<2EG	Total	<2 µm	Total		
KET-2	Ap-L. Alb	9.996	9.994	8.989	0.33	0.52	0.49	14.14	14.15	9.253	Ill-Sm
KET-3	Berr-Haut	9.999	9.990	8.999	0.50	0.52	0.40	14.13	14.13	9.249	Ill-Pg
KET-4	Berr-Haut	9.994	9.994	8.998	0.41	0.51	0.21	14.11	14.14	9,240	Ill/Sm, Pg
KET-5	Berr-Haut	9.982	10.007	8.995	0.41	0.40	0.40	14.10	14.13	9.270	
KET-6	Berr-Haut	10.007	10.006	8.994	0.47	0.47	0.42	14.12	14.13	9,275	Ill-Pg
KET-7	Berr-Haut	9.992	9.994	8.997	0.32	0.33	0.35	14.11	14.14	9.275	
KET-8	Aptian	10.015	9.965	8.997	0.41	0.46	0.37	14.14	14.13	9,250	Ill-Pg
KET-9	L. Albian	10.003	9.990	8.993	0.41	0.49	0.37	14.11	14.06	9,253	Pg
KET-10	L. Albian	10.005	10.011	8.994	0.57	0.48	0.49	14.12	14.14	9.250	Ill-Sm, Ill-Pg
TAO-4	Olig.	9.996	9.980	8.995	0.51	0.47	0.51	14.10	14.10	9.235	Ill-Sm

Mineral abbreviations according to Kretz (1983).
Ill-Sm= Illite-Smectite mixed-layers Ill-Pg= Na-K mica.
The high- and low-grade boundaries of anchizone in the "CIS" scale are 0.25 and 0.42º 2Θ (Merriman and Peacor, 1999).
Age abbreviations are: Brr-Haut: Berriasian–Hauterivian, Ap-L. Alb: Aptian–Lower Albian, L. Albian: Latest Albian, Olig.: Oligocene.

of phyllosilicates, quartz, and calcite (Fig. 3A, B, C, D, E). This slaty cleavage forms the main reference surface in the Tanger-Ketama sequence and is affected by asymmetric F2 folds. S1 shows no evidence in the outcrops or in thin sections of transposition cleavage, such as isolated hinges (Fig. 3B, C, D, E). The asymmetric folds (F2) have an axial plane foliation (S2) that is a crenulation cleavage in the Lower Cretaceous rocks (Berriasian–Hauterivian and Aptian–Lower Albian) and a discontinuous cleavage in the Jurassic and the uppermost Albian rocks. The S2 fabric is locally penetrative and developed mostly by solution-transfer mechanisms and the rotation of previous grains, as manifested by the presence of truncated stratigraphic layers (Fig. 3B, C), veins, and opaque mineral seams (Fig. 3B). In general, very little mineral growth is observed in relation with the S2-spaced crenulation cleavage (Fig. 3B). Foliation surfaces show NNW shallow dips and develop ENE-WSW-trending pencil structures in the pelites and metapelites. Moreover, locally, there is a gently dipping crenulation cleavage (S3) that deforms the first foliation in the rocks related to kink folds (Fig. 3F). The location of the areas with anchizone metamorphic conditions (Fig. 2) roughly coincides with the distribution of penetrative S1 and S2 foliations within the metapelitic rocks of the Tanger-Ketama Unit.

Figure 5 shows the geometry of the compressional structures of the Tanger- Ketama unit that deformed the S1 foliation (which formed in extensional conditions). The basal thrust surface of the Flysch units cut the reverse limb of the major F2 asymmetrical folds in the Lower Cretaceous phyllites and quartzites. There are three major synforms and three major antiforms with normal limbs with lengths of 4 to 6km and reverse limbs of 2km. F2 Folds have WSW-ENE trending hinges and vergences towards the SSE. The splay on top of the Jbel Tifoulest anticline has a ramp geometry in the footwall cutting the Jurassic and Berriasian–Hauterivian rocks and also the unconformable Upper Oligocene conglomerates, sandstones, and shales upwards towards the south. In Figure 4, Upper Miocene sediments of the Dhar Souk basin are unconformable on the afore-mentioned footwall rocks, whereas Lower Miocene rocks are cut by thrusts in the Jbel Taïneste area indicating that thrusts probably formed during the Early to Middle Miocene.

Serpentinite mineralogy and texture

The serpentinites show two main mineral assemblages, both recognizable at the optical and TEM scales (Fig. 3G, H). The first assemblage constitutes a mesh texture. The TEM data show that chrysotile, lizardite, and polygonal serpentine are in the mesh core and columnar lizardite is in the mesh rim (Fig. 7A, B, C). The second assemblage is a fine-grained antigorite aggregate alternating with the mesh textures along shear zones. Shear zones deformed the mesh structures, indicating that antigorite formed after the chrysotile, lizardite, and polygonal serpentine polymorphs. A modular structure, which is the unambiguously identifying characteristic of antigorite, is clearly visible in the lattice-fringe image and the electron diffraction diagram (Fig. 7D). The fine-grained antigorite aggregates consist of (001) twinned crystals (Fig. 7D). The aggregates show evidence of two kinds of reaction borders, one where antigorite replaces the mineral assemblage of the mesh texture and a second one where antigorite aggregates recrystallize to coarser grains.

The serpentinite assemblages support the occurrence of low-grade metamorphic evolution. In fact, the retrograde mesh-texture arrangements are well preserved and clearly visible at the optical scale. The transformation to antigorite is limited, localized, and associated with shearing. The whole mineralogy of serpentine and its textural pattern is strongly reminiscent of the serpentinites studied by Ribeiro da Costa *et al.* (2008) at the Mid-Atlantic ridge. These authors concluded that antigorite replaced chrysotile through dissolution-recrystallization. Such a process was favoured by shearing. According to oxygen isotope

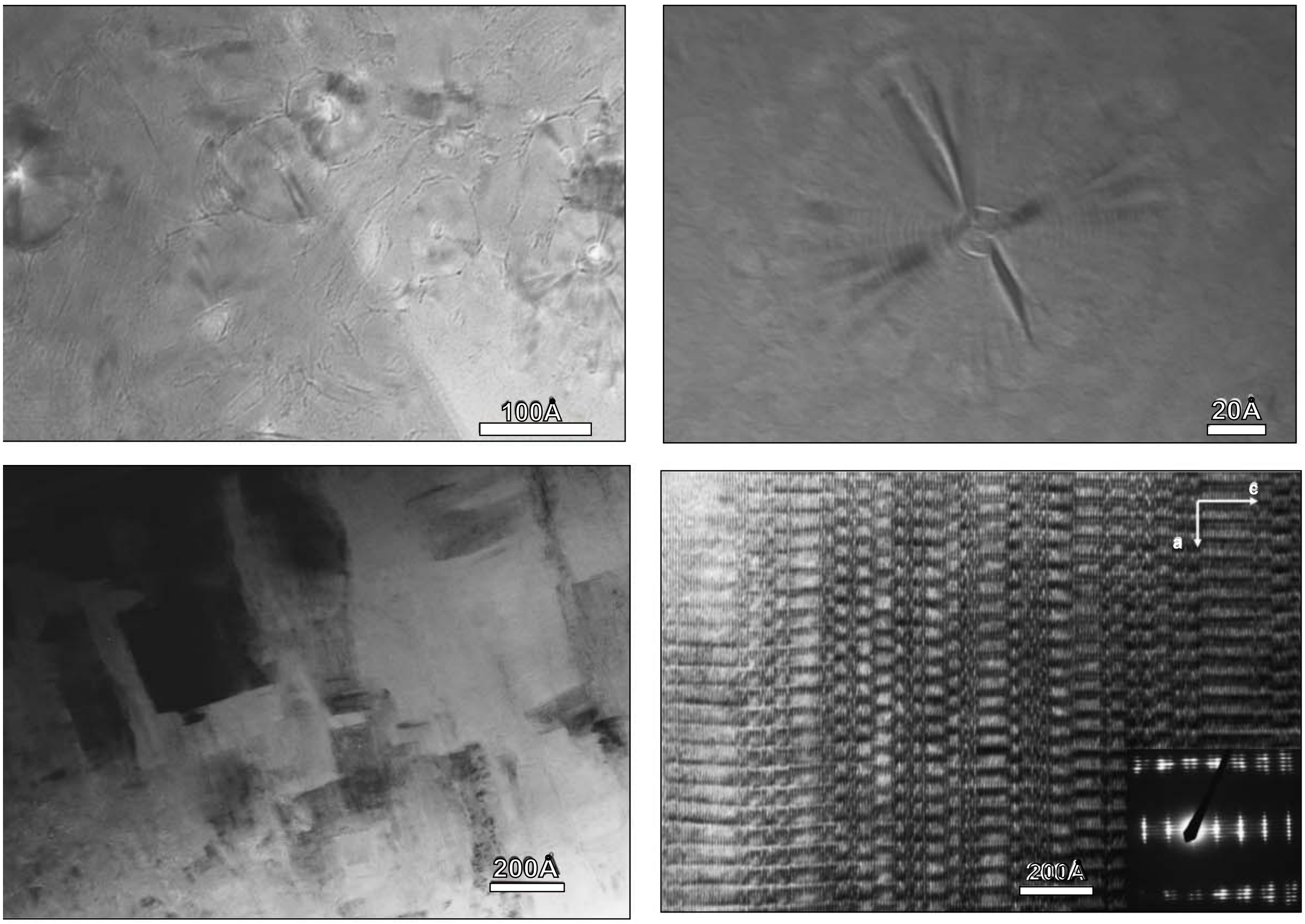

FIGURE 7 | TEM images of serpentine minerals. A and B: Mesh texture. A) Chrysotile showing its typical coiled structure and lizardite with a characteristic planar structure. B) Polygonal serpentine. C) Mesh rim (columnar lizardite). D) Lattice-fringe image of a (001) twinned antigorite crystal, with corresponding selected area electron diffraction (SAED) pattern in the inset.

temperatures, antigorite crystallization took place at temperatures between 200–300ºC. We propose a similar origin, where antigorite crystallized close to the antigorite-in reaction, possibly kinetically activated by deformation, as suggested by the association of antigorite to the shear zones.

DISCUSSION

The extensional metamorphism of the Tanger-Ketama Units

The distribution of illite crystallinity values and the mineralogical assemblages in the Tanger-Ketama metapelites indicate that near high anchizone conditions are located in the central part of the unit (Lower Cretaceous outcrops), whereas the deeper diagenetic conditions appear in the border units, where Upper Cretaceous or Jurassic rocks crop out. K-white mica dimensions range from 8.984 to 8.999Å, indicating the nearly pure muscovitic composition of micas, typical of the low-pressure conditions expected in an extensional low-grade setting, where shale sequences are buried in a passive margin scenario (Merriman and Frey, 1999; Merriman, 2005). According to Merriman (2005), extensional contexts typically have assemblages of clay minerals, including K-mica, Na-K, and Na-mica, together with lower b cell values (<9.01Å). In contrast, mud-rocks evolving in convergent settings have clay-mineral assemblages with K-white mica and chlorite, where the K-white micas have phengitic compositions with b cell dimensions of > 9.02Å (Merriman, 2005).

K/Ar and zircon fission track ages (Azdimousa *et al.*, 1998; 2003) indicate that the metamorphism was Cretaceous and prior to the known age of the compressional events in the Rif Belt (Cenozoic). Nevertheless, in the Jbel Tifelouest anticline, Jurassic rocks reached deeper diagenetic temperatures during 126.6±2.1Ma to 131.9±153.2Ma (Barremian), whereas in the central part of the Tanger-Ketama Unit, Cretaceous rocks reached temperatures close to high anchizone conditions from 78.0±1.2Ma to 81.6±4.0Ma (Campanian). This dichotomy in the K/Ar ages between the two areas, together with the higher grade reached at the latter, must be explained by an asymmetrical tectonic mechanism, both in geometry and time. As we discuss below, progressive extension and the development of asymmetric hanging-wall basins could account for the dichotomy in the age and the diagenetic to very low-grade metamorphic conditions in the area. These ages and the metamorphic conditions indicate that the Hauterivian to Lower Albian rocks in the area surrounding Bni Bounsar and Jbel Zercat were at lower levels and under thicker sediments than the Jurassic rocks of the Jbel Tifoulest area at around 80Ma. This geometry suggests that the entire sequence was tilted prior to 80Ma and, moreover, that the Cretaceous and younger sediments were thicker in the area near Bni Bounsar and Jbel Zercat than in the Jbel Tifoulest. This tilting is also suggested by the fact that, towards the east, Jurassic marbles increase in metamorphic degree and include bodies of greenschists and epidote-amphibolites in the Ait Amrâne klippe west of Midar (Fig. 2).

Significant extensional processes drove the exhumation of the mantle peridotites to seafloor conditions in the Early Cretaceous (140–145Ma) since the peridotites are stratigraphically overlain by Berriasian–Hauterivian rocks and the Tithonian carbonates form part of the pre-rift sequence. Such an extensional setting could explain the presence of the low-temperature polymorphs of serpentine (such as chrysotile, polygonal serpentine, and lizardite) in mesh textures and antigorite in shear zones formed from a spinel lherzolite in the Beni-Malek peridotites. Antigorite growth could occur during the low-temperature serpentinization or by the heating of the previously cooled peridotites by the Cretaceous sedimentary overburden. This last antigorite origin is supported by the low-grade metamorphism that affected the Jurassic marbles and greenschists in the Ait Amrâne klippe, where low-temperature peak metamorphic conditions were reached (<450ºC) at 80Ma (Jabaloy *et al*., 2012).

The presence of unconformable Oligocene detrital rocks with clasts from Mesozoic rocks of the Tanger-Ketama Unit indicates a period of exhumation and erosion of the Mesozoic Tanger-Ketama sequence during the Oligocene. As these clasts include the foliations developed within the Mesozoic rocks, they indicate that the compressive ductile deformations producing S2 and S3 foliations were generated before the Late Oligocene. Moreover, apatite fission-track ages indicate that the rocks cooled below 120ºC between 14 and 17Ma, probably from Alpine mountain range erosion during final emplacement. Altogether, these two facts suggest a period of post-Oligocene heating that raised the temperature to over 120ºC. This heating was probably related to the thrust sheet emplacement during the Early to Middle Miocene (Asebriy *et al*., 1992; Asebriy, 1994). However, the Miocene thrusting of the upper Ketama unit over the Oligocene conglomerates did not contribute to anchizonal metamorphism in the Ketama unit (Asebriy *et al*., 1992; Asebriy, 1994).

We propose a model for the basin where the Tanger-Ketama Unit sequence was deposited during the Mesozoic according to the conceptual diagram in Figure 8. This diagram was built using the cross-section in Figure 5 and data from Figures 2 and 4, although the lack of strain measurements makes an accurately balanced cross-section impossible. The easternmost part of the Tanger-Ketama unit (Fig. 2) is characterized by a lack of Jurassic rocks and by the presence of Lower Cretaceous rocks directly covering the Beni-Malek peridotites, whereas in the central and western parts of the unit, the Lower Cretaceous sediments overlie the Jurassic formations (Figs. 2; 4; 5). Towards the eastern Rif Chain, the Jurassic sediments overlie an extended Palaeozoic basement in one of the underlying Temsamane units, forming the Ras Afraou unit (*e.g*. Negro *et al*., 2007; Azdimousa *et al*., 2007). However, there is no evidence of rocks of a crustal basement for the Tanger-Ketama unit. The aeromagnetic data from Elazzab *et al*. (1997) (see Fig. 2) strongly indicate that the ultramafic rocks of the Beni-Malek peridotites continue below the outcrops of the Tanger-Ketama Lower Cretaceous rocks; and also that the ultramafics rocks have a tabular geometry at the base of the unit (Elazzab *et al*., 1997; Michard *et al*., 2007; Chalouan *et al*., 2008), as has been drawn in Figure 5.

The distribution of different types of basement of the tectonic unit and the aforementioned distribution of metamorphism (with a central part just under high-anchizone conditions bordered by diagenetic rocks) can be explained by a half-graben basin that was infilled by Cretaceous sediments under a high geothermal gradient. The progressive displacement and rotation of the hanging-wall above the extensional detachment and exhumed mantle would explain the dichotomy in the age of diagenetic conditions and the very low-grade metamorphism in the Jurassic and Cretaceous sediments of the Tanger-Ketama Unit.

In order to explain: i) the uplift of the Beni-Malek peridotitic body from spinel peridotite conditions to the seafloor, ii) the contact of the ultramafic body with the Lower Cretaceous sedimentary rocks, and iii) the presence of mafic- and also ultramafic-derived sandstones within the Lower Cretaceous sedimentary rocks southeast of the Beni-Malek massif (Michard *et al*., 1992; Chalouan *et al*., 2008), we propose the existence of a normal fault at the top of the ultramafic body allowing the uplift of the ultramafic rocks in the fault footwall. The faulting of the ultramafic rocks was followed by the later erosion of the fault surface on the seafloor in order to produce the ultramafic-derived

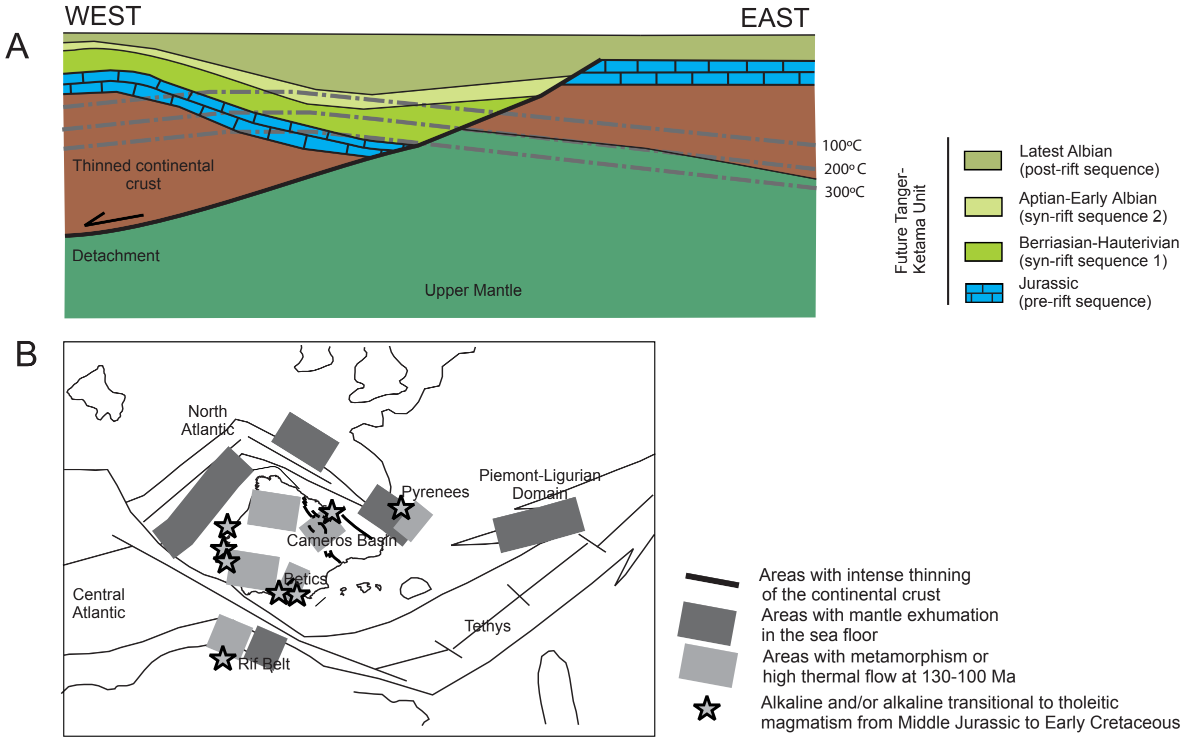

FIGURE 8 | A) Conceptual model for the geometry of the Tanger-Ketama basin during Upper Cretaceous times. The subcontinental mantle (spinel lherzolites) was covered by Cretaceous sediments, whereas the Jurassic pre-rift sequence was discontinuous. B) Location of the North African palaeomargin and its possible relationships with the Northern Atlantic Ocean opening around 105 Ma (Middle Albian), modified from Manatschal *et al.* (2006), with data from Stapel (1999), Mata *et al.* (2001), Jabaloy *et al.* (2002), Barbero and López-Garrido (2006), Terrinha *et al.* (2006), and Lagabrielle and Bodinier (2008).

sandstones and the geometry of a nonconformity for the top of the peridotite massif.

The Early Cretaceous rifting of the North Maghrebian passive margin: A comparison with the neighbouring peri-Iberian areas

Similar extensional environments formed during the Cretaceous in the Atlantic and Tethyan realms in the surrounding areas of the Iberian Peninsula between 117–92Ma (Albarède and Michard-Vitrac, 1978; Fabriés *et al.*, 1998; Mata *et al.*, 2001; Lagabrielle and Bodinier, 2008). In the Pyrenees, after an initial rifting phase in the Triassic to Late Jurassic that produced WNW-trending rift basins (Yilmaz *et al.*, 1996), a second rifting phase took place during the Aptian–Turonian (104–92Ma in the eastern Pyrenees, Albarède and Michard-Vitrac, 1978; 117–109Ma in the western Pyrenees, Fabriés *et al.*, 1998).

The second rifting phase in the Pyrenees produced the exhumation of spinel lherzolite massifs from upper mantle conditions to the seafloor of small Aptian–Albian basins (Fabriés *et al.*, 1998; Lagabrielle and Bodinier, 2008; Lagabrielle *et al.*, 2010). During the exhumation, peridotites cooled from circa 1050ºC to 600ºC (Fabriés *et al.*, 1998; Lagabrielle and Bodinier, 2008; Lagabrielle *et al.*, 2010). In the eastern Pyrenees, the ultramafic rocks induced high-temperature and low-pressure metamorphism in Triassic to Aptian–Albian sequences (T=550–650°C, P<3–4kbar; *e.g.* Montigny *et al.*, 1986; Golberg and Leyreloup, 1990). However, in the western Pyrenees, according to Fabriés *et al.* (1998), the exhumation of the ultramafic rocks at shallower levels compared to the massifs of the eastern Pyrenees, would explain the extensive hydrothermal alteration and serpentinization of the westernmost Pyrenean massifs. We propose that a similar mechanism to that of the exhumed ultramafic massifs in the western Pyrenees could also explain the emplacement of the Beni Malek ultramafic rocks. The major difference is that the Beni Malek peridotites probably cooled at around 300–400ºC when they reached the seafloor because we found no evidence of rocks metamorphosed under higher conditions than greenschist facies in the entire External Zones of the Rif Belt. One possible explanation is that exhumation in the North Maghrebian palaeomargin was slow and took a very long time, thereby allowing temperatures to equilibrate within the peridotitic body.

This period of time (ca. 122Ma) also corresponds to the timing of tectonic denudation and cooling of the mantle beneath the west Galician margin during the continental break-up between Iberia and Newfoundland (Boillot *et al*., 1987; Schärer *et al*., 1995), and to the emplacement of mantle peridotites that at present are exposed on the seafloor in other areas near the western Tethys realm (*e.g*. Discovery 215 Working Group, 1998; Reston *et al*., 1996; Hölker *et al*., 2002; Manatschal *et al*., 2006), indicating that this process was not exclusive to the Pyrenean realm.

Moreover, in the continental rocks of the Iberian Peninsula, fission tracks in apatites recorded the existence of a heating period in the Early Cretaceous (*e.g*. Stapel, 1999; Barbero and López-Garrido, 2006; Martín-González *et al*. 2006) accompanied by the intrusion of mafic rocks (Boillot and Malond, 1988; Féraud *et al*., 1988; Schärer *et al*., 1995) and hydrothermal processes (Caballero *et al*., 1992). Juez-Larré and Ter Voorde (2009) compiled thermochronological data of the Iberian Peninsula and determined that several heating stages during the Mesozoic (including one heating phase during the Early Cretaceous) produced the resetting of thermochronometers with closure temperatures of up to 200°C and the increase of the geothermal gradient up to ~73°C/km. These facts agree with the observed apatite fission-track ages in the Tanger-Ketama rocks and the increase in the geothermal gradient in the study area during the same period.

In summary, the presence of exhumed spinel lherzolites on the seafloor accompanied by metamorphism of the overlying sediments in a high geothermal gradient in the Maghrebian palaeomargin during the Aptian–Albian is a plausible scenario that can explain both the very low-grade metamorphism and the thermochronological ages of the rocks of the Tanger-Ketama Unit.

CONCLUSIONS

Our study shows that diagenetic conditions and anchizonal very low- to low-grade metamorphism affected parts of the External Zones of the Rif Belt. Illite crystallinity of white mica shows diagenetic to anchizone conditions within the metapelites. Greenschist and epidote-amphibolite mineral assemblages within Jurassic marble in the Ait Amrâne klippen and possibly antigorite growth in serpentinites indicate that low-grade metamorphism was attained. K/Ar and zircon fission track ages (Azdimousa *et al*., 1998; 2003) indicate that the anchizone conditions of this extensional metamorphism were reached during the Campanian (ca. 80Ma), whereas diagenetic conditions were reached at 130Ma.

The structure of the deduced North African palaeomargin during the Cretaceous must have been similar to that described in the western Galician non-volcanic passive margin, where the syn-rift sediments were deposited in half-graben basins above an exhumed serpentinized mantle and extended Palaeozoic basement. Our study shows a metamorphic pattern for the External Zones of the Rif Belt, where initial metamorphism was generated during the Cretaceous related to burial within a half-graben asymmetric basin, suggesting an extensional setting.

Finally, Tertiary Alpine metamorphism and deformation in the Tanger-Ketama Unit were not high enough to overprint the Cretaceous extensional metamorphism and reset the K/Ar and fission-track clocks.

ACKNOWLEDGMENTS

We acknowledge the financial support of Research projects “CSD2006-0041 “TOPO-IBERIA” (CONSOLIDER-INGENIO program of the Ministerio de Ciencia e Innovación, Gobierno de España), Excelencia Project RNM-327 (Junta de Andalucía Government), AECI A/5904/06 and A/010149/07 and Research Group RNM-148 of the Junta de Andalucía. We would also like to thank the Research Unit associated with CNRST (URAC 46) Morocco, for logistical support and equipment for field work and sampling. We would like to thank F. Nieto for his assistance in the interpretation of the Kübler Index and the serpentine minerals. We would also like to thank A. Crespo-Blanc, Y. Lagabrielle, D.M. Poyatos, and J.D. Barrenechea for fruitful discussions regarding this work. Thanks are also given to Christine Laurin for revising the English text.

REFERENCES

Andrieux, J., 1971. La structure du Rif Central, Notes du Service Géologique du Maroc, 235.

Asebriy, L., 1994. Evolution tectonique et métamorphique du Rif Central (Maroc): Définition du domaine subrifain, Doctoral Thesis. University of Rabat, Morocco, 248pp.

Asebriy, L., Azdimousa, A., Bourgois, J., 2003. Structure du Rif externe sur la trnsversale du Massif de Kétama. Travaux de l’Institut Scientifique, Rabat, Maroc, 21, 27-46.

Asebriy, L., Bourgois, J., De Luca, P., Butterlin, J., 1992. Importance d’une tectonique de distension Pliocène dans le Rif Central (Maroc): La nappe de Kétama existe-t-elle?. Jounal of African Earth Sciences, 15, 49-57.

Asebriy, L., De Luca, P., Bourgois, J.; Chotin, P., 1987. Resédimentation d’âge Sénonien dans le Rif Central (Maroc): Conséquences sur les divisions paléogeographiques et structurales de la chaîne. Journal of African Earth Sciences, 6, 9-17.

Azdimousa, A., Bourgois, J., Asebriy, L., Poupeau, G., Montigny, R., 2003. Histoire thermique et surrection du Rif externe et des nappes de flyschs associées (Nord Maroc), Travaux de l’Institut Scientifique, Rabat, 21, 15-26.

Azdimousa, A., Bourgois, J., Poupeau, G., Montigny, R., 1998. Histoire thermique du massif de Kétama (Maroc); sa place en Afrique du Nord et dans les cordillières Bétiques. Comptes Rendus de l'Académie des Sciences de Paris, 326, 847-853.

Azdimousa, A., Jabaloy, A., Asebriy, L., Booth-Rea, G., González-Lodeiro, F., Bourgois, J., 2007. Lithostratigraphy and structure of the Temsamane unit (Eastern external Rif, Morocco). Revista de la Sociedad Geológica de España, 20(3-4), 187-200.

Balanyá, J.C., García-Dueñas, V., 1987. Les directions structurales dans le Domaine d'Álboran de part et d'autre du L'Étroit de Gibraltar. Comptes Rendus de l'Académie des Sciences de Paris, 304 (Serie II), 929-932.

Barbero, L., López-Garrido, A.C., 2006. Mesozoic thermal history of the Prebetic continental margin (southern Spain): Constraints from apatite fission-track analysis. Tectonophysics, 422, 115-128.

Boillot, G., Froitzheim, N., 2001. Non-volcanic rifted margins, continental break-up and the onset of sea-floor spreading: Some outstanding questions. In: Wilson, R. C. L., Whitmarsh, R.B., Taylor, B., Froitzheim, N. (eds.) Non-Volcanic Rifting of Continental Margins: A Comparison of Evidence from Land and Sea. London Geological Society, 187 (Special Publications), 9-30.

Boillot, G., Malond, J., 1988. The north and north-west Spanish continental margin: a review. Revista de la Sociedad Geológica de España, 1, 295-317.

Boillot, G., Recq, M., Winterer, E.L., Meyer, A.W., Applegate, J., Baltuck, M., Bergen, J.A., Comas, M.C., Davies, T.A., Dunham, K., Evans, C.A., Girardeau, J., Goldberg, G., Haggerty, J., Jansa, L.F., Johnson, J.A., Kasahara, J., Loreau, J.P., Luna-Sierra, E., Moullade, M., Ogg, J., Sarti, M., Thurow, J., Williamson, M., 1987. Tectonic denudation of the upper mantle along passive margin: A model based on drilling results (Ocean Drilling Program Leg 103, Western Galicia Margin, Spain). Tectonophysics, 132, 335-342.

Bourgois, J., 1977. D'une étape géodynamique majeure dans la genèse de l'arc de Gibraltar: "L'hispanisation des flyschs rifains au Miocène inférieur". Bulletin de la Société Géologique de la France, XIX, 115-1119.

Caballero, J. M., Casquet, C., González-Casado, J. M., Snelling, N., Tornos, F., 1992. Dating of hydrothermal events in the Sierra de Guadarrama, Iberian Hercynian Belt, Spain. Geogaceta, 11, 18-21.

Casas, A. M., Cortés, A. L., Maestro, A., 2000. Intra-plate deformation and basin formation in the northern Iberian plate: Origin and evolution of the Almazán Basin. Tectonics, 19, 258-289.

Chalouan, A., Michard, A., 2004. The Alpine Rif belt (Morocco): A case of mountain building in a subduction-subduction-transform fault triple junction. Pure and Applied Geophysics, 161(3), 489-519.

Chalouan, A., Michard, A., El Kadiri, Kh., Negro, F., Frizon de Lamotte, D., Soto, J. I., Saddiqi, O., 2008. Chapter 5. The Rif Belt. In: Michard, A., Saddiqi, O., Chalouan, A., Frizon de Lamotte, D. (eds.). Continental Evolution: The Geology of Morocco. Structure, Stratigraphy, and Tectonics of the Africa-Atlantic-Mediterranean Triple Junction. 116, Springer-Verlag Berlin Heidelberg, Lecture Notes in Earth Sciences, 203-302.

Choubert, G., Faure-Muret, A., Hilali, E. A., Houzay, J. P., Frizon de Lamotte, D., 1984. Carte géologique du Rif, échelle 1/50000, feuille Boudinar. Notes et Mémories du Service Géologique du Maroc, 299.

Ciszak, R., 1987. Resédimentation intrasénonienne du Trias évaporitique dans le sillon tellien (Algérie). Implications dans la tectogenèse des Maghrébides. Géologie Mediterranéenne XIV, 137-141.

Ciszak, R., Magne, J., Peybernes, B., 1986. Interprétation du complexe chaotique "triasique" d´Oraine (Algérie occidentale) comme un olistostrome sénonien localement réinjecté dans les accidents alpins. Comptes Rendus de l'Académie des Sciences de Paris, 402, 357-362.

Dewey, J. F., Helman, M. L., Turco, E., Hutton, D. H., Knot, S. D. 1989. Kinematics of the western Mediterranean. In: Coward, M.P., Dietrich, D., Park, R.G. (eds.). Conference on Alpine tectonics, 45, 265-283.

Discovery 215 Working Group, 1998. Deep structure in the vicinity of the ocean-continent transition zone under the southern Iberia Abyssal Plain. Geology 26, 743-746.

Durand-Delga, M., Hottinger, L., Marcais, J., Mattauer, M., Milliard, Y., Suter, G., 1962. Données actuelles sur la structure du Rif. Livre à la mémoire du professeur Fallot. Mémoires hors série, Paris, Société Géologique de la France, 1. 399-442.

Duran-Delga, M., Rossi, P., Olivier, P., Puglisi, D., 2000. Situation structurale et nature ophiolitique de roches basiques jurassiques associées aux flyschs maghrébins du Rif (Maroc) et de Sicile (Italie). Comptes Rendus de l'Académie des Sciences, de Paris, 331 (1, Series II), 29-38.

Elazzab, D., Galdeano, A., Feinberg, H., Michard, A., 1997. Prolongement en profondeur d'une écaille ultrabasique allochtone: traitement des donnéees aéromagnétiques et modélisation 3D des péridotites des Beni Malek (Rif, Maroc). Bulletin de la Société Géologique de la France, 168, 667-683.

Fabriés, J., Lorand, J. P., Bodinier, J.L., 1998. Petrogenetic evolution of orogenic lherzolite massifs in the central and western Pyrenees. Tectonophysics, 292, 145-167. doi:10.1016/S0040-1951(98)00055-9

Faccenna, C., Piromallo, C., Crespo-Blanc, A., Jolivet, L., Rossetti, F., 2004. Lateral slab deformation and the origin of the western Mediterranean arcs. Tectonics, 23(TC1012). doi:10.1029/2002TC001488.

Féraud, G., Girardeau, J., Beslier, M. O., Boillot, G., 1988. Datation $^{39}Ar/^{40}Ar$ de la mise en place des péridotites bordant la marge de la Galice (Espagne). Comptes Rendus de l'Académie de Sciences de Paris, 307 (Series II), 49-55.

Frizon de Lamotte, D., 1985. La structure du Rif oriental (Maroc). Rôle de la tectonique longitudinale et importance des fluides. Mémoires des Sciences de la Terre, University Paul et Marie Curie, Paris VI. Doctoral Thesis.

Goldberg, J. M., Leyreloup, A. F., 1990. High temperature–low pressure Cretaceous metamorphism related to crustal thinning (eastern north Pyrenean zone, France). Contributions to Mineralogy and Petrology, 104, 194–207. doi: 10.1007/BF00306443

Goldberg, J. M., Guiraud, M., Malusky, H., Séguret, M., 1988. Caractères pétrologiques et âge du métamorphisme en context distensif du basin sur décrochement de Soria (Crétacé inférieur, Nord Espagne). Comptes Rendus de l´Académie des Sciences de Paris, 307, 521-527.

Goldberg, J.M., Maluski, H., Leyreloup, A.F., 1986. Petrological and age relationship between emplacement of magmatic breccia, alkaline magmatisme, and static metamorphism in the North Pyrenean Zone. Tectonophysics, 129, 275-290.

Gübeli, A., Hochuli, P. A., Wildi, W., 1984. Lower Cretaceous turbiditic sediment from the Rif chain (northern Morocco), palynology, stratigraphy setting. Geologisches Rundschau, 73, 1081-1114.

Guidotti, C. V., Sassi, F. P., 1986. Classification and correlation of metamorphic facies series by means of muscovite b0 data from low-grade metapelites. Neues Jahrbuch fur Mineralogie, Abhandlungen, 153, 363-380.

Harmand, C. H., Asebriy, L., De Luca, P., 1988. Un témoin de l'évolution géodynamique du Rif central (Maroc) au cours du Mésozoïque: l'intrusion alcaline de Bou Adel. Clermont-Ferrand, 11ème Réunion des Sciences de la Terre, Société Géologique de la France.

Hölker, A., Holliger, K., Manatschal, G., Anselmetti, F., 2002. Seismic structure of the Iberian and Tethyan distal continental margins based on geological and petrophysical data. Tectonophysics, 350, 127-156.

Jabaloy, A., Booth-Rea, G., Azdimousa, A., Asebriy, L., Vázquez, M., Martínez-Martínez, J. M., Gabites, J., 2012. $^{40}Ar/^{39}Ar$ constraints on the activity of the Temsamane extensional detachment (eastern Rif, Morocco). Geophysical Research Abstracts, 14, EGU2012-7792.

Jabaloy, A, Galindo-Zaldívar, J., González-Lodeiro, F., 2002. Palaeostress evolution of the Iberian Peninsula (Late Carboniferous to present-day). Tectonophysics, 357, 159-186.

Jolivet, L., Faccenna, C., Goffé, B., Burov, E., Agard, P., 2003. Subduction tectonics and exhumation of high-pressure metamorphic rocks in the Mediterranean orogens. American Journal of Science, 303, 353-409.

Juez-Larré, J., Ter Voorde, M., 2009. Thermal impact of the break-up of Pangea on the Iberian Peninsula, assessed by thermochronological dating and numerical modeling. Tectonophysics, 474, 200–213, doi: 10.1016/j.tecto.2009.01.024

Kisch, H. J., 1991. Illite 'crystallinity': Recommendations on sample preparation, X-ray diffraction settings and interlaboratory samples. Journal of Metamorphic Geology, 9, 665-670.

Kisch, H. J., Arcai, P., Brime, C., 2004. On the calibration of the illite Kübler index (illite crystallinity). Schweizerische Mineralogische und Petrographische Mitteilungen, 84, 323-331.

Kretz, R., 1983. Symbols for rock-forming minerals. American Mineralogist, 68, 277-279.

Kuhnt, W., Obert, D., 1991. Evolution crétacée de la marge tellienne. Bulletin de la Sociéte Géologique de la France, 162, 515-522.

Lagabrielle, Y., Bodinier, J. L., 2008. Submarine reworking of exhumed subcontinental mantle rocks: Field evidence from the Lherz peridotites, French Pyrenees. Terra Nova, 20(1), 11-21, doi: 10.1111/j.1365-3121.2007.00781.x

Lagabrielle, Y., Labaume, P., de Saint Blanquat, M., 2010. Mantle exhumation, crustal denudation, and gravity tectonics during Cretaceous rifting in the Pyrenean realm (SW Europe): Insights from the geological setting of the lherzolite bodies. Tectonics, 29, TC4012. doi: 10.1029/2009TC002588

Leblanc, D., 1975-1979. Etude géologique du Rif externe oriental au Nord de Taza (Maroc). Notes et Mémoires du Service Géologique du Maroc, 281.

Leikine, M., Asebriy, L., Bourgois, J., 1991. Sur l'âge du métamorphisme anchiépizonal de l'unité de Kétama, Rif central (Maroc). Comptes Rendus de l'Académie des Sciences de Paris, 313,787-793.

Lespinasse, P., 1975. Géologie des zones externes et des flyschs entre Chaouen et Zoumi (Centre de la chaîne rifaine, Maroc). Doctoral Thesis, Université Paul et Marie Curie, Paris VI.

Manatschal, G., Engström, A., Desmur, L., Schaltegger, U., Cosca, M., Muentener, O., Bernoulli, D., 2006. What is the tectono-metamorphic evolution of continental break-up: The example of the Tasna Ocean-Continent Transition. Journal of Structural Geology, 28, 1849-1869.

Martín-González, F., Capote, R., Barbero, L., Insua, J. M., Martínez-Díaz, J. J., 2006. Primeros resultados de huellas de fisión en apatito en el sector Lugo-Ancares (Noroeste de la Península Ibérica). Geogaceta, 40, 79-82.

Massonne, H. J., Schereyer, W., 1987. Phengite geobarometry based on the limiting assemblage with K-feldspar, phlogopite and quartz. Contributions to Mineralogy and Petrology, 96, 212-224.

Massonne, H.J., Szpurka Z., 1997. Thermodynamic properties of white micas on the basis of high-pressure experiments in the systems K_2O-MgO-$A_{12}O_3$-SiO_2-H_2O and K_2O-FeO-Al_2O_3-SiO_2-H_2O. Lithos, 41, 229-250.

Mata, M. P., Casas, A. M., Canals, A., Gil, A., Pocovi, A., 2001. Thermal history during Mesozoic extension and Tertiary uplift in the Cameros basin, northern Spain. Basin Research, 13, 91-11.

Merriman, R. J., 2005. Clay minerals and sedimentary basin history. European Journal of Mineralogy, 17, 7-20.

Merriman, R.J., Frey, M., 1999. Patterns of very low-grade metamorphism in metapelitic rocks. In: Frey, M., Robinson, D. (eds.). Low-grade metamorphism. Oxford, Blackwell Science, 61-107

Merriman, R.J., Peacor, D.R., 1999. Very low-grade metapelites: mineralogy, microfabrics and measuring reaction progress. In: Frey, M., Robinson, D. (eds.). Low-grade metamorphism. Oxford, Blackwell Science, 10-60.

Merriman, R.J., Roberts, B., 1985. A survey of white mica crystallinity and polytypes in pelitic rocks of Snowdonia and Llyn, N. Wales. Mineralogical Magazine, 49, 305-319.

Michard, A., Feinberg, H., El-Azzab, D., Bouybaouène, M., Saddiqi, O., 1992. A Serpentinite ridge in a collisional paleomargin setting: The Beni Malek Massif, external Rif, Morocco. Earth and Planetary Science Letters, 113(3), 425-442.

Michard, A., Frizon de Lamotte, D., Negro, F., Saddiqui, O., 2007. Serpentinite slives and metamorphism in the external Maghrebides: Arguments for an intracontinental suture in the African paleomargin (Morocco, Algeria). Revista de la Sociedad Geológica de España, 20, 173-185.

Michard, A., Negro, F., Saddiqi, O., Bouybaouène, M. L., Chalouan, A., Montigny, R., 2006. Pressure-temperature-time constraints on the Maghrebide mountain building: Evidence from the Rif-Betic transect (Morocco), Algerian correlations, and geodynamic implications. Comptes Rendus Géoscience, 338(1-2), 92-114.

Monié, P., Frizon de Lamotte, D., Leikine, M., 1984. Etude géochronologique préliminaire par la méthode 39Ar/40Ar du métamorphisme alpin dans le Rif externe (Maroc); précisions sur le calendrier tectonique tertiaire. Revue de Géologie Dynamique et de Géographie Physique, 25(4), 307-317.

Montigny, R., Azambre, B., Rossy, M., Thuizat, R., 1986. K-Ar study of Cretaceous magmatism and metamorphism in the Pyrenees: Age and length of rotation of the Iberian Peninsula. Tectonophysics, 129, 257-273, doi:10.1016/0040-1951(86)90255-6

Nieto, F., Mata, P., Bauluz, B., Giorgetti, G., Árkai, P., Peacor, D. R., 2005. Retrograde diagenesis, a wide spread process on a regional scale. Clay Minerals, 40, 93-104.

Negro, F., 2005. Exhumation des roches métamorphiques du Domaine d'Alborán: étude de la chaîne rifaine et corrélation avec les Cordillères Bétiques. Doctoral Thesis. Paris, Université Paris XI, France, 91pp.

Negro, F., Agard, P., Goffé, B., Saddiqi, O., 2007. Tectonic and metamorphic evolution of the Temsamane units, External Rif (northern Morocco): Implications for the evolution of the Rif and the Betic-Rif arc. London, Journal of the Geological Society, 164, 829-842.

Negro, F., de Sigoyer, J., Goffé B., Saddiqi, O., Villa, I. M., 2008. Tectonic evolution of the Betic–Rif arc: New constraints from $^{40}Ar/^{39}Ar$ dating on white micas in the Temsamane units (External Rif, northern Morocco). Lithos, 106, 93-108. doi:10.1016/j.lithos.2008.06.011

Pérez-Gussinyé, M., Reston, T. J., 2001. Rheological evolution during extension at nonvolcanic rifted margins: Onset of serpentinization and development of detachments leading to continental breakup. Journal of Geophysical Research, 106(B3), 3, 961-963, 975.

Reston, T. J., Krawczyk, C. M., Klaeschen, D., 1996. The S reflector west of Galicia: Evidence from prestack depth migration for detachment faulting during continental break-up. Journal of Geophysical Research, 101, 8075-8091.

Ribeiro Da Costa, I., Barriga, F., Viti, C., Mellini, M., Wicks, F. J., 2008. Antigorite in deformed serpentinites from the Mid-Atlantic Ridge. European Journal of Mineralogy, 20, 563-572.

Roberts, B., Merriman, R. J., 1985. The distinction between Caledonian burial and regional metamorphism in metapelites from North Wales: An analysis of isocryst pattern, Journal of the Geological Society, London, 142, 625-624.

Robinson, D., 1987. Transition from diagenesis to metamorphism in extensional and collision settings. Geology, 15, 866-869.

Robinson, D., Bevins, R.E., 1986. Incipient metamorphism in the Lower Palaeozoic marginal basin of Wales. Journal of Metamorphic Geology, 4, 101-113.

Robinson, D., Bevins, R. E., 1989. Diastathermal (extensional) metamorphism at very low grades and possible high grade analogues. Earth and Planetary Science Letters, 92, 81-88.

Sassi, F. P., Scolari, A., 1974. The b0 value of the potassic white mica in low-grade metamorphism rocks. An application to eastern Alps. Tschermaks Mineralogische und Petrographische Mitteilungen, 18, 105-113.

Schärer, U., Kornprobst, J., Beslier, M. O., Boillot, G., Girardeau. J., 1995. Gabbro and related rock emplacement beneath rifting continental crust: U–Pb geochronological and geochemical constraints for the Galicia passive margin (Spain). Earth and Planetary Science Letters, 130, 187-200.

Stapel, G., 1999. The nature of isostasy in western Iberia. Doctoral thesis, Vrije Universiteit, Amsterdam.

Sutter, G., 1980. Carte structurale de la chaîne rifaine à 1/500000. Notes et Mémoires du Service Géologique du Maroc.

Terrinha, P., Rocha, R., Rey, J., Cachão, M., Moura, D., Roque, C., Martins, L., Valadares, V., Cabral, J., Azevedo, M.R., Barbero, L., Clavijo, E., Dias, R.PO., Gafeira, J., Matias, H., Matias, L., Madeira, J., Marques da Silva, C., Munhá, J., Rebêlo, L., Ribeiro, C, Vicente, J., Youbi, N., 2006. A Bacia do Algarve: Estratigrafia, Paleogeografia e Tectónica. In: Dias, R., Araújo, A., Terrinha, P., Kullberg (eds.). Geologia de Portugal no contexto da Ibéria (Universitdade de Évora, Portugal), 247-316.

Vidal, J.F., 1971. Une interprétation nouvelle des nappes du Prérif central (Maroc) et ses conséquences sur la structure de leur substratum autochtone. Comptes Rendus de l'Académie des Sciences de Paris, 272, 24-27.

Warr, L. N., Rice, A. H. N., 1994. Interlaboratory standardization and calibration of clay mineral crystallinity and crystallite size data. Journal of Metamorphic Geology, 12, 141–152.

Wilson, R. C., Whitmarsh, R. B., Froitzheim, N., Taylor, B., 2001. Introduction: the land and sea approach. In: Wilson, R. C., Whitmarsh, R. B., Taylor, B., Froitzheim, N. (eds.). Non-Volcanic Rifting of Continental Margins: A Comparison of Evidence from Land and Sea. Geological Society, London, Special Publications, 187, 1-8. doi:10.1144/GSL.SP.2001.232.01.28

Yilmaz, P. O., Norton, I. O., Leary, D., Chuchla, R. J., 1996. Tectonic evolution and paleogeography of Europe. In: Ziegler, P.A., Horvàth, F. (eds.). Peri-thetis Memoir 2: Structure and Prospects of Alpine Basins and Forelands. Muséum National d'Histoire Naturelle, Paris (France), Publications Scientifiques, 47-60.

Zhang, Y. K., 1993. The thermal blanketing effect of sediments on the rate and amount of subsidence in sedimentary basins formed by extension. Tectonophysics, 218(4), 297-308

Manuscript received May 2011;
revision accepted November 2012;
published Online January 2013.